ADVANCED FUNCTIONAL MATERIALS
www.afm-journal.de

Polyethylene Imine as an Ideal Interlayer for Highly Efficient Inverted Polymer Light-Emitting Diodes

*Young-Hoon Kim, Tae-Hee Han, Himchan Cho, Sung-Yong Min, Chang-Lyoul Lee, and Tae-Woo Lee**

Electron-injecting interlayers (ILs) which are stable in air, inject electrons efficiently, block holes, and block quenching of excitons, are very important to realize efficient inverted polymer light-emitting diodes (IPLEDs). Two air-stable polymer electron-injecting interlayers (ILs), branched polyethyleneimine (PEI) and polyethyleneimine ethoxylated (PEIE) for use in IPLEDs are introduced, and the roles of the ILs in IPLEDs comparing these with a conventional Cs_2CO_3 IL are elucidated. These polymer ILs can reduce the electron injection barrier between ZnO and emitting layer by decreasing the work function (WF) of underlying ZnO, thereby effectively facilitating electron injection into the emitting layer. WF of ZnO covered by PEI is found to be lower than that covered by PEIE due to higher [N^+]/[C] ratio of PEI. Furthermore, they can block the quenching of excitons and increase the luminous efficiency of devices. Thus, IPLEDs with PEI IL of optimum thickness (8 nm) show current efficiency (13.5 cd A^{-1}), which is dramatically higher than that of IPLEDs with a Cs_2CO_3 IL (8 cd A^{-1}).

1. Introduction

Polymer light-emitting diodes (PLEDs) are promising for large-area displays and solid state lighting sources due to many advantages including ease and low cost of fabrication, large-area application and the possibility of fabrication using the roll-to-roll process.[1] Although luminous efficiency and lifetime of PLEDs have been increased, their air-sensitive electron injection materials (e.g., Ca, LiF) still limit the viability of PLEDs as displays and lighting sources. These air-sensitive electron injection materials make device fabrication impossible in air and induce rapid device degradation. They also induce the increase of fabrication cost due to the necessity of depositing them under high vacuum. Thus, the conventional structure of PLEDs has been a critical obstacle for roll-to-roll mass production at a low cost. Therefore, inverted structure PLEDs (IPLEDs) having air-stable metal oxide as an electron injection layer have been proposed as a novel structure which solve those air-sensitivity problems.[2–10]

In IPLEDs, inorganic n-type metal oxides, such as titanium oxides (TiO_x),[3–6] zirconium dioxide (ZrO_2),[5] and zinc oxide (ZnO)[4,8–10] have been evaluated as electron injection materials due to their air-stability, solution processability, transparency to visible light, and tunable electrical-optical properties. ZnO has been most widely investigated due to its n-type property resulting from interstitial Zn atom and oxygen vacancies.[2,7,11,12] However, ZnO has a high electron injection barrier into the emitting layer (EML) because the lowest unoccupied molecular orbital (LUMO) energy level of ZnO (≈4.4 eV) is much deeper than the LUMO (2.8–3.2 eV) of the EML.[13] This large electron injection energy barrier (≈1.2–1.6 eV) impedes electron injection into the EML and limits overall electron-hole balance. Furthermore, the metallic nature of ZnO induces electron-hole exciton dissociation[14–17] which reduces device efficiency. Employing a thin caesium carbonate (Cs_2CO_3) interlayer (IL) on the ZnO can induce an interfacial dipole and thereby reduce the work function (WF) of ZnO.[8,9] Therefore, the electron injection barrier from ZnO to EML is reduced and electrons can be injected easily. Furthermore, decomposed Cs^+ ions can facilitate electron injection by doping EML to n-type[18,19] and can also form a hole-blocking layer.[20] However, the air-sensitivity of Cs_2CO_3 limits its feasibility in roll-to-roll processes,[21] and Cs^+ ions that diffuse into a polymer EML can form exciton quenching sites.[13] An interfacial layer should be stable in air, inject electrons efficiently, block holes, and block quenching of excitons.

This paper reports two air-stable polymer ILs for IPLEDs: branched polyethyleneimine (PEI) and polyethyleneimine ethoxylated (PEIE) which can induce efficient electron injection as well as efficient blocking of holes and blocking of exciton quenching. **Figure 1** presents the structure of IPLEDs and chemical structure of PEI and PEIE. These polymers are composed of amine groups in their backbone and side chains, and can therefore cause a strong molecular dipoles not only within the structure but also between an adsorbed PEI molecule and the under-lying ZnO surface.[22] These strong dipoles can shift the vacuum level and reduce the WF of ZnO, and can reduce the electron injection energy barrier to make electron injection into

Y.-H. Kim, T.-H. Han, H. Cho, S.-Y. Min, Prof. T.-W. Lee
Department of Materials Science and Engineering
Pohang University of Science and Technology (POSTECH)
Pohang, Gyungbuk 790-784, Republic of Korea
E-mail: twlee@postech.ac.kr
Dr. C. -L. Lee
Advanced Photonics Research Institute (APRI)
Gwangju Institute of Science & Technology (GIST)
1 Oryong-dong
Buk-gu, Gwangju 500-712, Korea

DOI: 10.1002/adfm.201304163

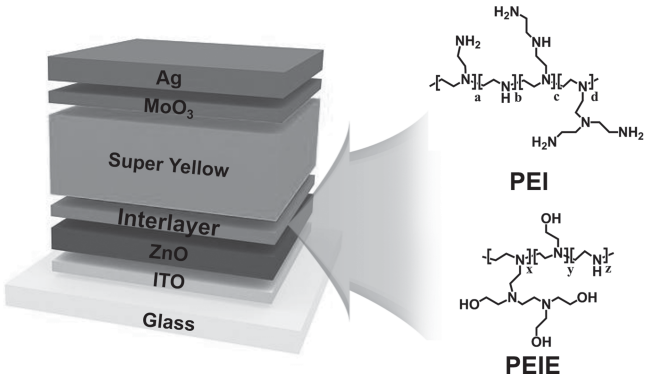

Figure 1. The IPLEDs structure using PEI and PEIE on ZnO layer.

the EML more efficiently than that use Cs_2CO_3. We also found that the electron injection barrier and the WF of ZnO tend to increase with increasing polymer IL thickness and studied the effect of the $[N^+]/[C]$ ratios of the two polymer ILs on the WF of ZnO. Furthermore, polymer ILs also efficiently block holes and block quenching of excitons that occur at the interface between ZnO and EML. In addition, quenching of excitons tends to gradually decrease with increasing polymer IL thickness and to saturate at around ≈10-nm thickness. Finally, in IPLEDs with optimum IL thickness and an 8-nm PEI layer, we achieved high current efficiency (13.5 cd A^{-1}) which were higher than that obtained using a Cs_2CO_3 IL (8 cd A^{-1}). Our device architecture enables non-vacuum roll-to-roll processed IPLEDs with improved luminous efficiency because polymer ILs lack all the drawbacks (e.g., air-sensitivity) of commonly-used charge injection layers (e.g., Cs_2CO_3, LiF) in PLEDs, but facilitate electron injection, blocking of holes and blocking of exciton quenching.

2. Results and Discussion

To study how the polymer ILs reduced the electron injection barrier, we used ultraviolet photoelectron spectroscopy (UPS) to measure the WFs of samples with ZnO (22 nm)/no IL, Cs_2CO_3 IL, PEI IL (4, 8, 12, 16 nm) (**Figure 2**a), PEIE IL (4, 8, 12, 16 nm) (Figure 2b). PEI (2.47 eV at 4 nm) and PEIE (3.29 eV at 4 nm) both shifted the WF of ZnO (4.4 eV) much more than did Cs_2CO_3 (3.56 eV) due to the strong interfacial dipole induced by the large number of amine groups in their structure (**Table 1**). The considerable reduction in the WF of ZnO with polymer IL (≈2.47 eV for 4 nm PEI) can greatly reduce the electron injection barrier more than can ZnO/ Cs_2CO_3 (WF ≈ 3.56 eV). These reduced electron injection barrier facilitated easier electron injection into the EML and established efficient electron-hole balance in the device.

As the thickness of PEI and PEIE increased, the WF of ZnO gradually increased from 2.47 eV (4 nm PEI) to 3.39 eV (16 nm PEI) and from 3.29 eV (4 nm PEIE) to 3.6 eV (16 nm PEIE). These changes indicate that as the thickness of the polymer ILs increases, randomly oriented dipoles gradually countervail each other and the interfacial dipole between ZnO and ILs gradually decreases as a consequence. Thus, the electron injection barrier between ZnO and EML increases and electron injection capability decreases with polymer IL thickness. To characterize

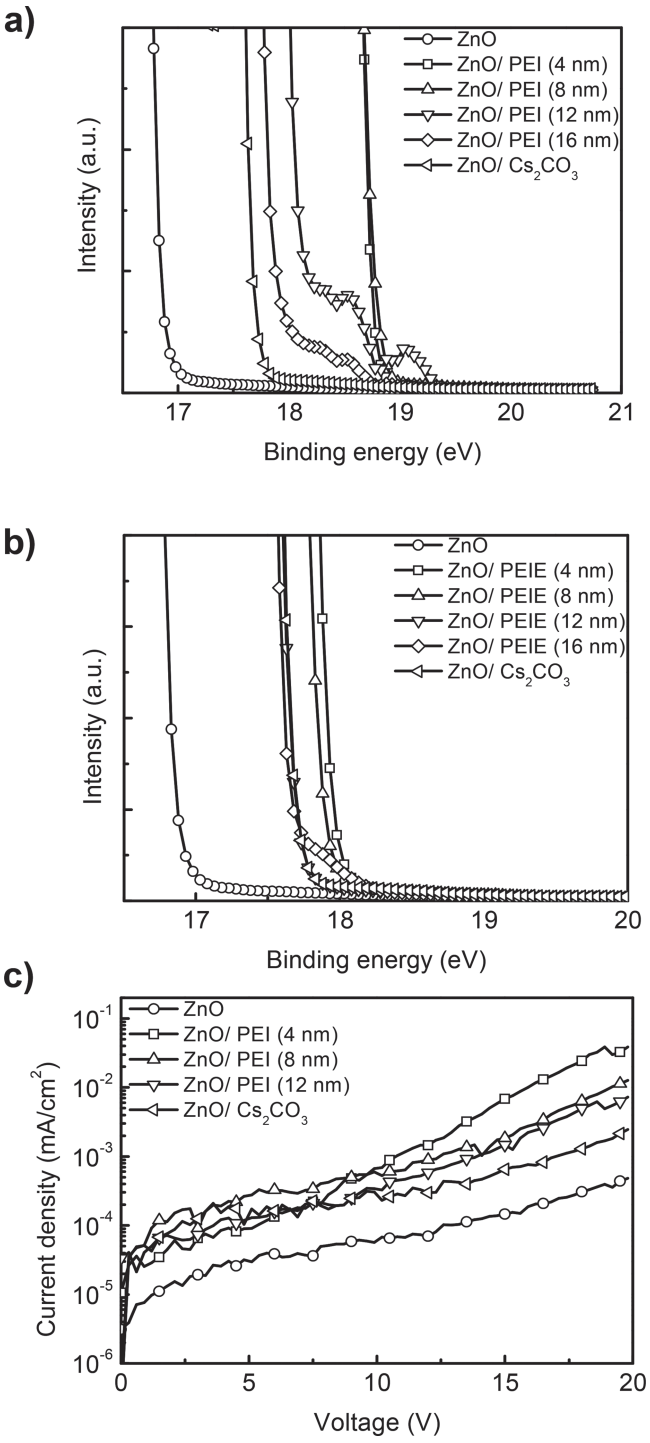

Figure 2. a) UPS spectra of ZnO, ZnO/Cs_2CO_3, and ZnO/PEI (4 nm, 8 nm, 12 nm, and 16 nm). b) UPS spectra of ZnO, ZnO/Cs_2CO_3, and ZnO/PEIE (4 nm, 8 nm, 12 nm, and 16 nm). c) Current density versus voltage characteristics of electron-only devices; ITO/ZnO/no interlayer, Cs_2CO_3, and PEI (4 nm, 8 nm, and 12 nm)/super yellow/Ca/Al.

the increased electron injection capability and thickness effects of polymer ILs on devices, we fabricated electron-only devices with ITO/ ZnO/no IL, Cs_2CO_3 IL, PEI IL (4, 8, 12 nm)/super yellow (SY) (≈230 nm)/Ca (3 nm)/Al (120 nm) and measured

Table 1. Work function of ZnO with no interlayer, Cs_2CO_3, PEIE, and PEI.

Thickness	ZnO	ZnO/Cs_2CO_3	ZnO/PEIE	ZnO/PEI
	4.4 eV	3.56 eV		
4 nm			3.29 eV	2.47 eV
8 nm			3.36 eV	2.44 eV
12 nm			3.55 eV	3.17 eV
16 nm			3.6 eV	3.39 eV

current density (Figure 2c). Electron-only devices with a 4-nm PEI IL showed current density 80 times higher than devices with no IL, but devices with a Cs_2CO_3 IL showed current density only 5 times higher than devices with no IL at 20 V. As PEI thickness increased, electron current density gradually decreased; this trend was coincident with UPS spectra (Table 1). In addition to the increased WF arising from randomly-oriented dipoles in the thick IL, increased insulating polymer thickness makes electron injection into the EML difficult.

PEI reduced the WF of ZnO more than did PEIE at every IL thickness. To prove this fact, we conducted quantitative X-ray photoelectron spectroscopy (XPS) analysis. Because the intensity of an interfacial dipole is attributed to protonated amines which induce electrostatic dipoles, and to carbon atoms which interrupt self-assembly of protonated amines in a polymer ILs,[23] we compared the [N^+]/[C] ratios of ZnO/ PEI (8 nm) and ZnO/PEIE (8 nm). In XPS spectra, ZnO/PEI and ZnO/PEIE showed clear carbon 1s peaks near 286 eV, and nitrogen 1s peaks that correspond to protonated (401 eV) and non-protonated (399.5 eV) amines (**Figure 3**a).[24–26] Compared to PEIE, XPS spectra of PEI showed a slightly higher nitrogen peak and a similar carbon peak. Furthermore, PEI had proportionally much more protonated amines than did PEIE (Figures 3b,c). ZnO/PEI had higher [N^+]/[C] ratio (≈0.207) than did ZnO/PEIE (≈0.135); this means that ZnO/PEI has more protonated amines than does ZnO/PEIE, so ZnO/PEI can therefore induce stronger electrostatic dipoles on the ZnO surface than can ZnO/PEIE. These differences result from the larger number of N atoms in the PEI polymer chain than in the PEIE chain. Thus, more N atoms in PEI than in PEIE can adsorb onto the ZnO surface and be easily protonated. Therefore, PEI causes a stronger electrostatic dipole and a deeper reduction of the WF of ZnO than does PEIE.

In IPLED structure (ITO/ZnO/IL/SY/MoO_3/Ag), a recombination zone can form at the ZnO/SY interface due to ohmic contact in SY/MoO_3/Ag and 1.5 times higher hole mobility of SY than electron mobility.[27,28] Thus, in devices with no IL which can block holes and block exciton quenching, the metallic nature of ZnO induces exciton dissociation.[14–17] Therefore, an IL that can block holes and block exciton quenching at the ZnO surface of the ZnO/SY interface is needed. To study the effect on quenching of excitons occurring on ZnO surface of polymer ILs, we conducted time-correlated single-photon counting (TCSPC) with different polymer ILs to obtain the fluorescence lifetime change of the EML film and steady-state PL with various thickness of PEI to study the thickness effect on quenching of excitons of polymer IL. We fabricated various samples of glass/ no IL, PEIE IL (8 nm), PEI IL (8 nm)/SY (≈10 nm)

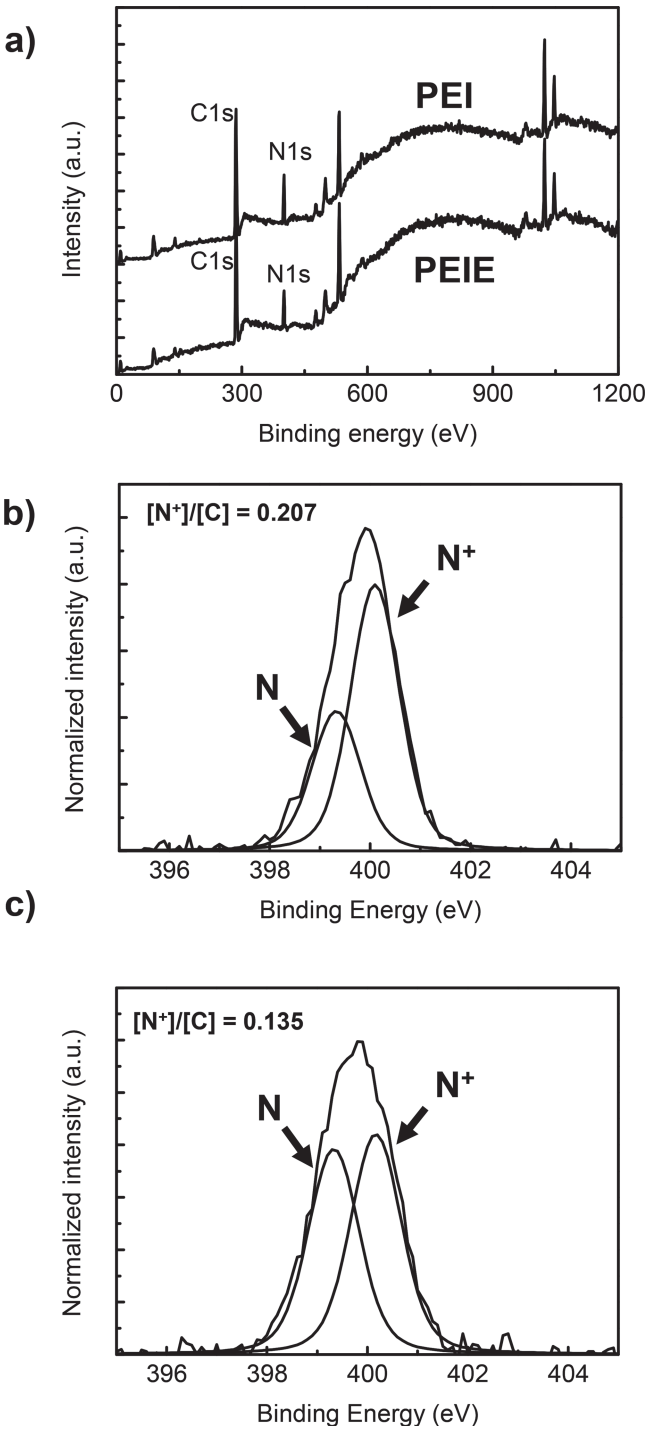

Figure 3. a) XPS spectra of ZnO/PEIE and ZnO/PEI, b) N (1s) response in XPS spectra of ZnO/PEI, c) N (1s) response in XPS spectra of ZnO/PEIE.

and conducted TCSPC measurements (**Figure 4**a). Very thin polymer ILs can block exciton quenching. Fluorescence lifetime from ZnO/PEI/SY (0.45 ns) and ZnO/PEIE/SY (0.42 ns) were much higher than that from ZnO/SY (0.34 ns) (**Table 2**). These increases of fluorescence lifetime obtained by inserting PEI and PEIE indicate that quenching of excitons is reduced

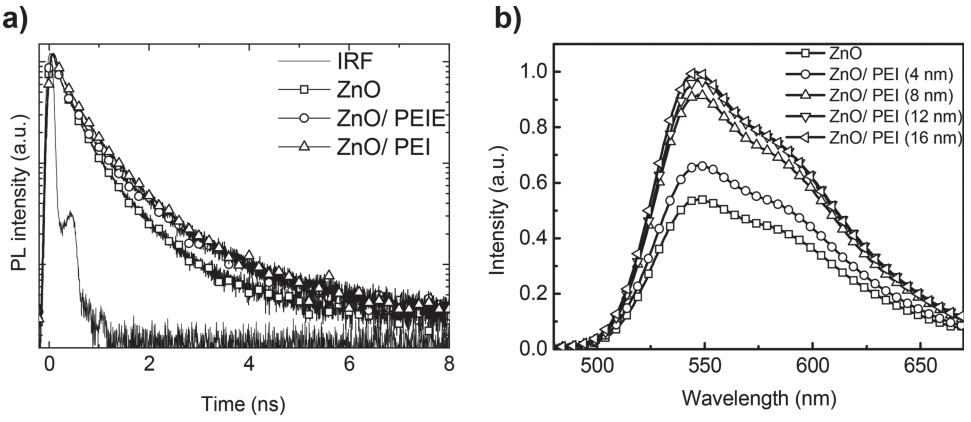

Figure 4. a) PL lifetime curves obtained from time-correlated single photon counting measurement (TCSPC) of super yellow (≈10 nm) on different under-layers in ZnO, ZnO/PEIE (8 nm) and ZnO/PEI (8 nm). The lifetime was monitored at 550 nm; τ_{avr} is average lifetime from $f_1\tau_1 + f_2\tau_2$, where f_1 and f_2 are fractional intensities and τ_1 and τ_2 are measured lifetimes, respectively). b) Photoluminescence (PL) intensities of super yellow (≈10 nm) on ZnO/PEI (0 nm, 4 nm, 8 nm, 12 nm, and 16 nm).

and radiative decay of excitons is increased. Furthermore, PEI showed slightly longer fluorescence lifetime than did PEIE, which means that PEI can block holes and block quenching of excitons more efficiently than can PEIE. This difference can be ascribed to two mechanisms of exciton quenching: exciton dissociation at the surface driven by the large energy level difference between the LUMO (≈2.82 eV) of SY and the WF of the underlying ZnO layer; and non-radiative energy transfer from SY to metallic ZnO.[29,30]

Energy differences between LUMO of SY and ZnO, ZnO/PEIE (8 nm) and ZnO/PEI (8 nm) were 1.65 eV, 0.61 eV, and 0.31 eV, respectively. Because exciton dissociation was caused by energy level difference, fluorescence lifetimes tended to decrease with the relative energy level difference between the LUMO of SY and the WF of the underlayer. Fluorescence lifetime was shortest (0.34 ns) in ZnO/SY with the largest energy level difference (1.65 eV), intermediate (0.42 ns) in ZnO/PEIE (8 nm)/SY (0.61 eV), and longest (0.45 ns) in ZnO/PEI (8 nm) (0.31 eV); this trend implies that compared to PEIE, PEI blocks exciton quenching more efficiently.

Steady state PL results in samples with glass/no IL, PEI IL (4, 8, 12, 16 nm)/SY (≈10 nm) showed the thickness effect on blocking of exciton quenching of PEI occurring on ZnO/ SY interface (Figure 4b). Increasing the thickness of PEI caused the intensities of PL peak to gradually increase and to saturate at ≈10-nm PEI thickness; this trend is due to the increasing distance between generated excitons and the quenching ZnO interface as the PEI increases, and to the estimated exciton diffusion length in SY film (≈10 nm).[31–33] We did not observe any PL spectrum change of the thin SY film with polymer ILs and with a Cs_2CO_3 IL from that with no IL; because the polymer ILs did not affect the chain orientation of SY, but just changed the surface properties of ZnO (Supporting Information, Figure S1).

Table 2. PL lifetimes obtained from TCSPC of super yellow on different under-layers in ZnO, ZnO/ PEIE (8 nm) and ZnO/ PEI (8 nm).

Polymer film	$\tau_1(f_1)$ [ns]	$\tau_2(f_2)$ [ns]	χ^2	τ_{avr} [ns]
ZnO/Super Yellow	0.83 (0.17)	0.24 (0.83)	1.585	0.34
ZnO/PEIE/Super Yellow	1.07 (0.19)	0.27 (0.81)	1.735	0.42
ZnO/PEI/Super Yellow	1.07 (0.19)	0.31 (0.81)	1.712	0.45

Atomic force microscopy (AFM) measurements of ZnO surface with different thickness of PEI IL, a Cs_2CO_3 IL and no IL indicated that the PEI IL gradually reduced the roughness of ZnO with increasing thickness of PEI IL (Supporting Information Figure S2). Root-mean-squared (RMS) roughness values of the ZnO surface decreased from 4.28 nm in the ZnO film to 0.737 nm in the ZnO/PEI (16 nm) film; this means that PEI IL can flatten the peaks on the ZnO surface. Thus, PEI can reduce the leakage current caused by these peaks. PEIE also showed similar surface morphology improvement (Supporting Information, Figure S3). However, ZnO/ Cs_2CO_3 (Supporting Information, Figure S2b) showed increased RMS (≈5.72 nm) and many peaks > 80 nm tall; these protruding peaks can induce leakage current in IPLEDs.

Relationships of current density (mA cm^{-2}) with respect to voltage (V) of the IPLEDs with different ILs and with no IL showed that the devices with PEI and PEIE exhibit lower threshold voltages (V_{th}), above which current density increases rapidly, that were 1.5 V and 2.5 V, respectively, than that of device with Cs_2CO_3 (≈3 V) (**Figure 5**a). Furthermore, devices with polymer ILs showed much higher current density under high V than did devices with the Cs_2CO_3 IL and with no IL. These high current density and low V_{th} in devices with polymer ILs demonstrate convincingly that polymer ILs can effectively reduce the electron injection barrier and facilitate electron injection into EML; these conclusions are coincident with UPS data and electron-only devices (Table 1; Figure 2). This result is consistent with previous research that shows that electron injection is dominantly influenced by the surface WF rather than by layer conductivity although it has a thin insulating layer.[34–37] However, IPLEDs with no IL showed no clear V_{th} and low current density under high V due to the absence of a hole-blocking/ electron injection IL. At voltages < V_{th}, IPLEDs with a PEI IL and with a PEIE IL showed low leakage current

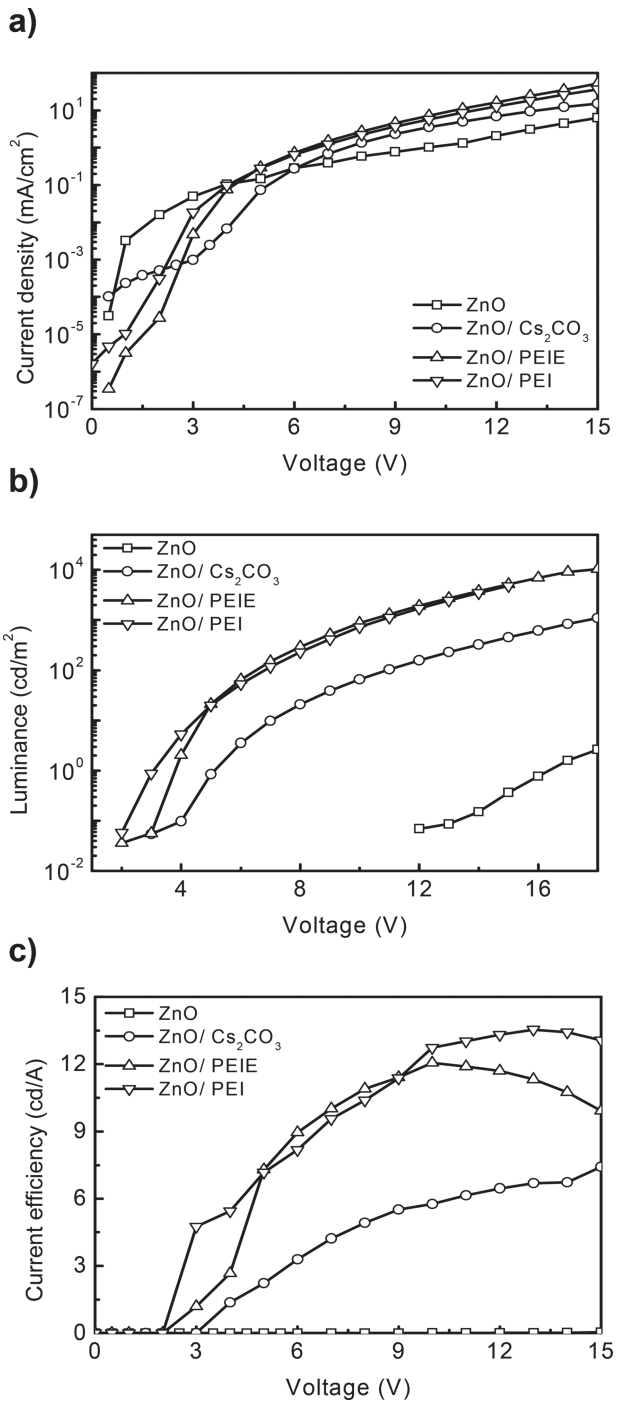

Figure 5. a) Current density versus voltage characteristics of inverted PLEDs with no interlayer, Cs_2CO_3, PEIE, and PEI, b) luminance versus voltage characteristics of inverted PLEDs with no interlayer, Cs_2CO_3, PEIE, and PEI, and c) current efficiency versus voltage characteristics of inverted PLEDs with no interlayer, Cs_2CO_3, PEIE, and PEI.

due to reduced surface roughness of ZnO and hole-blocking capability (Supporting Information, Figures S2,S3). Devices without an IL showed relatively high leakage current due to the high electron injection barrier between ZnO and EML, and to the absence of a hole-blocking layer. Devices with a Cs_2CO_3 IL showed the highest leakage current: although Cs_2CO_3 can act as a hole-blocking/ electron injection interlayer, increased surface roughness in ZnO/Cs_2CO_3 induced such high leakage current. The turn-on voltage (voltage at 1 cd m^{-2}) and operating voltage (voltage at 1000 cd m^{-2}) of IPLEDs using a PEI IL (≈3 V/≈10 V) and a PEIE IL (≈3.8 V/≈10 V) were much lower than those with a Cs_2CO_3 IL (≈5.14 V/18 V) and with no IL (≈16.3 V turn-on voltage) (Figure 5b). These results were attributed to the increased electron injection and increased blocking of exciton quenching by polymer ILs.

The current efficiency (CE) versus voltage characteristics were measured for IPLEDs with different ILs and with no IL (Figure 5c). Devices with a PEI IL had CE ≈13.5 cd A^{-1} and devices with a PEIE IL had CE ≈12 cd A^{-1}; these were much higher than those of the devices with a Cs_2CO_3 IL (≈8 cd A^{-1}) and with no IL (≈0.08 cd A^{-1}); this improvement indicates that our polymer ILs have excellent capability for electron-injection, blocking of holes and blocking of exciton quenching. The slightly higher CE of devices with a PEI IL compared to devices with a PEIE IL can be ascribed to better electron injection capability (Table 1) and blocking of exciton quenching capability (Figure 4a) of PEI compared to PEIE. The improved CE in the device with PEI indicates that PEI has excellent capability to inject electrons and to block hole/ exciton quenching, which are important factors for increasing CE in an IPLED device with emitting polymer having higher hole mobility than electron mobility, because CE is closely related to efficient exciton recombination without exciton quenching at the ZnO/EML interface.

Current densities and luminance of IPLEDs with a PEI IL gradually decreased as the thickness of the PEI IL increased (**Figures 6**a, b). As PEI thickness increased, turn-on voltage and operating voltage tended to gradually increase, but maximum luminance tended to gradually decrease. These trends are due to the increase in the electron injection barrier as the PEI IL thickness increases, as confirmed by UPS data. The CE of the device using 8-nm PEI (≈13.5 cd A^{-1}) was greater than those of devices that used other thicknesses of PEI: 4 nm (≈8.5 cd A^{-1}), 12 nm (≈13.1 cd A^{-1}) and 16 nm (≈5.04 cd A^{-1}). This non-linear trend indicates that a trade-off occurs between decreasing electron injection capability and increasing blocking of exciton quenching capability as PEI thickness increase, and that the optimum thickness for IPLEDs is ≈8 nm.

We also tested the device lifetime with initial luminance at 500 cd m^{-2} for the device using PEI and Cs_2CO_3 as an electron injection IL (Supporting Information, Figure S4). The half-lifetime of the device with PEI (20 h at 500 cd m^{-2}) increased dramatically compared with the half-lifetime of the device with Cs_2CO_3 (1 h at 500 cd m^{-2}). While the Cs_2CO_3 is intrinsically very unstable to moisture and oxygen, PEI is stable to moisture and oxygen. Therefore, the greatly increased lifetime can be ascribed to the more environmentally-stable characteristics of the PEI interlayer as well as the enhanced device efficiency resulting in lower driving current density at the same luminance.

3. Conclusions

We have demonstrated an efficient and air-stable IPLEDs by employing two kinds of amine-group-based polymers as an IL

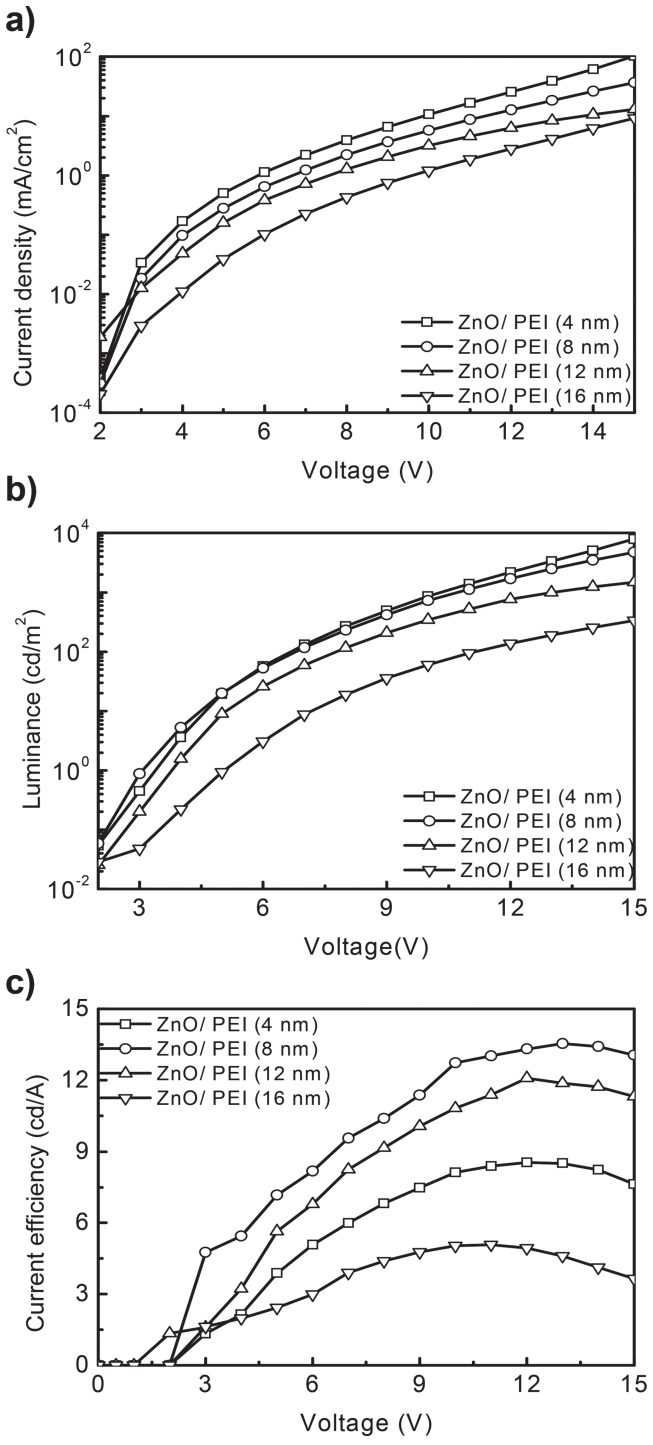

Figure 6. a) Current density versus voltage characteristics of inverted PLEDs with PEI (4 nm, 8 nm, 12 nm, and 16 nm) b) luminance versus voltage characteristics of inverted PLEDs with PEI (4 nm, 8 nm, 12 nm, and 16 nm), and c) current efficiency versus voltage characteristics of inverted PLEDs with PEI (4 nm, 8 nm, 12 nm, and 16 nm).

between ZnO and EML, and achieved a much improved CE (≈13.5 cd A^{-1} for device with PEI, ≈12 cd A^{-1} with PEIE) comparing with IPLEDs with Cs_2CO_3 IL (≈8 cd A^{-1}). These polymer ILs significantly reduce the WF of ZnO and the electron injection barrier by inducing a strong interfacial dipole. We also used quantitative XPS measurements to quantify how the $[N^+]/[C]$ ratio in PEI and PEIE affects the WF of ZnO, and used TCSPC to determine that the insulating polymer interlayers blocks quenching of excitons at the ZnO/EML interface where electrons recombine with holes in IPLEDs that have an dominantly hole-transporting emitting layer (SY). We used UPS to demonstrate gradual increase of WF of ZnO and used PL to demonstrate the decrease of exciton quenching with increasing IL thickness. Therefore, efficient radiative-recombination of holes with electrons at the ZnO/EML interface can be achieved by using an IL with optimum thickness. Our work suggests that the IL in IPLEDs should consider three important factors: 1) air-stability, 2) efficient electron injection, and 3) efficient blocking of holes and of exciton quenching at the EIL/EML interface. This strategy that uses an air-stable polymer IL in IPLEDs can reduce the fabrication cost due to the feasibility of processing in air, and can increase the radiative recombination related to both increasing electron injection into the EML and blocking of exciton quenching. Because, according to the scientific and technological roadmaps which suggest that future flexible OLEDs will be commercialized by PLEDs, our strategy using an insulating polymer IL for simultaneous electron injection and blocking of exciton quenching suggests that large-area displays and solid state lighting can be realized by using IPLEDs.

4. Experimental Section

OLED Fabrication: Indium-tin-oxide (ITO) coated substrates were sonicated twice in acetone and once in isopropanol for 15 min each. They were boiled in isopropanol for 15 min to remove the residue, then dried on a hot plate. On the pre-cleaned ITO coated glass, ZnO was deposited by sputtering to give 22-nm thickness. Then the ITO with deposited ZnO UV-ozone treated for 30 min to increase its hydrophilicity. PEI and PEIE dissolved in 2-methoxythanol were spin cast onto ZnO to give layers of 4 nm, 8 nm, 12 nm, and 16 nm and then was dried at 100 °C for 10 min in air. The substrates were transferred into a glove box and Super Yellow (Merck OLED Materials. GmbH, catalog number PDY-132) dissolved in toluene was spin cast onto the PEI interface layer to give a 230-nm layer. The device was annealed at 80 °C for 20 min, then transferred to a high-vacuum chamber (<10^{-7} Torr), in which MoO_3 (5 nm) (powder, 99.99%, Sigma-Aldrich) and Ag (50 nm) was deposited as the anode.

OLED Characterization: The current-voltage-luminance (*I–V–L*) characteristics were measured using a Keithley 236 source measurement unit and a Minolta CS2000 Spectroradiometer.

Photoluminescence (PL) Measurement: PL spectra were measured using a JASCO FP6500 spectrofluorometer. The wavelength of excitation light was 450 nm.

Time-Correlated Single Photon Counting (TCSPC) Measurement: PL decays of Super Yellow on diffferent substrate were investigated by the Time-Correlated Single Photon Counting (TCSPC) measurement. The second harmonic (SHG = 420 nm) of a tunable Ti:sapphire laser (Mira900, Coherent) with ≈150 fs pulse width and 76MHz repetition rate was used as an excitation source. The PL emission was spectrally resolved by using some collection optics and a monochromater (SP-2150i, Acton). The TCSPC module (PicoHarp, PicoQuant) with a MCP-PMT (R3809U-59, Hamamatsu) was used for ultrafast detection. The total instrument response function (IRF) for PL decay was less than 140 ps and the temporal time resolution was less than 10 ps. The deconvolution of actual fluorescence decay and IRF was performed by using a fitting software (FlouFit, PicoQuant) to deduce the time

constant associated with each exponential decay. All measurements are performed under ambient conditions.

Supporting Information

Supporting Information is available from the Wiley Online Library or from the author.

Acknowledgements

This work was supported by a grant (Code No.2013M3A6A5073175) from the Center for Advanced Soft Electronics under the Global Frontier Research Program of the Ministry of Science, ICT & Future Planning, Korea. This work was also supported by the National Research Foundation of Korea(NRF) grant funded by the Korea government (MSIP) (NRF-2013R1A2A2A01068753).

Received: December 13, 2013
Revised: February 5, 2014
Published online: March 10, 2014

[1] J. H. Burroughes, D. D. C. Bradley, A. R. Brown, R. N. Marks, K. Mackay, R. H. Friend, P. L. Burns, A. B. Holmes, *Nature* **1990**, *347*, 539.
[2] H. J. Bolink, E. Coronado, D. Repetto, M. Sessolo, *Appl. Phys. Lett.* **2007**, *91*, 223501.
[3] H. J. Bolink, E. Coronado, D. Repetto, M. Sessolo, E. M. Barea, J. Bisquert, G. Garcia-Belmonte, J. Prochazka, L. Kavan, *Adv. Funct. Mater.* **2008**, *18*, 145.
[4] D. Kabra, M. H. Song, B. Wenger, R. H. Friend, H. J. Snaith, *Adv. Mater.* **2008**, *20*, 3447.
[5] N. Tokmoldin, N. Griffiths, D. D. C. Bradley, S. A. Haque, *Adv. Mater.* **2009**, *21*, 3475.
[6] K. Morii, M. Ishida, T. Takashima, T. Shimoda, Q. Wang, Md. K. Nazeeruddin, M. Grätzel, *Appl. Phys. Lett.* **2006**, *89*, 183510.
[7] T.-W. Lee, J. Hwang, S.-Y. Min, *ChemSusChem* **2010**, *3*, 1021.
[8] M. H. Song, D. Kabra, B. Wenger, R. H. Friend, H. J. Snaith, *Adv. Funct. Mater.* **2009**, *19*, 2130.
[9] J. S. Park, B. R. Lee, E. Jeong, H.-J. Lee, J. M. Lee, J.-S. Kim, J. Y. Kim, H. Y. Woo, S. O. Kim, M. H. Song, *Appl. Phys. Lett.* **2011**, *99*, 163305.
[10] B. R. Lee, H. Choi, J. S. Park, H. J. Lee, S. O. Kim, J. Y. Kim, M. H. Song, *J. Mater. Chem.* **2011**. *21*. 2051.
[11] Y. W. Heo, D. P. Norton, S. J. Pearton, *J. Appl. Phys.* **2005**, *98*, 073502.
[12] Ü. Özgür, Y. I. Alivov, C. Liu, A. Teke, M. A. Reshchikov, S. Doğan, V. Avrutin, S.-J. Cho, H. Morkoç, *J. Appl. Phys.* **2005**, *98*, 041301.
[13] D. Kabra, L. P. Lu, M. H. Song, H. J. Snaith, R. H. Friend, *Adv. Mater.* **2010**, *22*, 3194.
[14] D. C. Olson, Y.-J. Lee, M. S. White, N. Kopidakis, S. E. Shaheen, D. S. Ginley, J. A. Voigt, J. W. P. Hsu, *J. Phys. Chem. C* **2007**, *111*, 16640.
[15] T. C. Monson, M. T. Lloyd, D. C. Olson, Y.-J. Lee, J. W. P. Hsu, *Adv. Mater.* **2008**, *20*, 4755.
[16] D. C. Olson, Y.-J. Lee, M. S. White, N. Kopidakis, S. E. Shaheen, D. S. Ginley, J. A. Voigt, J. W. P. Hsu, *J. Phys. Chem. C* **2008**, *112*, 9544.
[17] Q. Zheng, G. Fang, F. Cheng, H. Lei, W. Wang, P. Qin, H. Zhou, *J. Phys. D: Appl. Phys.* **2012**, *45*, 455103.
[18] H.-H. Liao, L.-M. Chen, Z. Xu, G. Li, Y. Yang, *Appl. Phys. Lett.* **2008**, *92*, 173303.
[19] Y. Vaynzof, D. Kabra, L. L. Chua, R. H. Friend, *Appl. Phys. Lett.* **2011**, *98*, 113306.
[20] H. J. Bolink, E. Coronado, J. Orozco, M. Sessolo, *Adv. Mater.* **2009**, *21*, 79.
[21] Y. W. Park, J. H. Choi, T. H. Park, E. H. Song, H. Kim, H. J. Lee, S. J. Shin, B.-K. Ju, W. J. Song, *Appl. Phys. Lett.* **2012**, *100*, 013312.
[22] Y. Zhou, C. F.-Hernandez, J. Shim, J. Meyer, A. J. Giordano, H. Li, P. Winget, T. Papadopoulos, H. Cheun, J. Kim, M. Fenoll, A. Dindar, W. Haske, E. Najafabadi, T. M. Khan, H. Sojoudi, S. Barlow, S. Graham, J.-L. Brédas, S. R. Marder, A. Kahn, B. Kippelen, *Science* **2012**, *336*, 327.
[23] H. Kang, S. Hong, J. Lee, K. Lee, *Adv. Mater.* **2012**, *24*, 3005.
[24] Y. Chen, E. T. Kang, K. G. Neoh, S. L. Lim, Z. H. Ma, K. L. Tan, *Colloid Polym. Sci.* **2001**, *279*, 73.
[25] E. Metwalli, D. Haines, O. Becker, S. Conzone, C. G. Pantano, *J. Colloid Interface Sci.* **2006**, *298*, 825.
[26] R. Schlapak, D. Armitage, N. Saucedo-Zeni, G. Latini, H. J. Gruber, P. Mesquida, Y. Samotskaya, M. Hohage, F. Cacialli, S. Howorka, *Langmuir* **2007**, *23*, 8916.
[27] M. Kröger, S. Hamwi, J. Meyer, T. Riedl, W. Kowalsky, A. Kahn, *Org. Electron.* **2009**, *10*, 932.
[28] S. R. Tseng, Y. S. Chen, H. F. Meng, H. C. Lai, C. H. Yeh, S. F. Horng, H. H. Liao, C. S. Hsu, *Synth. Met.* **2009**, *159*, 137.
[29] J.-S. Kim, R. H. Friend, I. Grizzi, J. H. Burroughes, *Appl. Phys. Lett.* **2005**, *87*, 023506.
[30] J. Mei, M. S. Bradley, V. Bulović, *Phys. Rev. B* **2009**, *79*, 235205.
[31] T. Stübinger, W. Brütting, *J. Appl. Phys.* **2001**, *90*, 3632.
[32] D. E. Markov, E. Amsterdam, P. W. M. Blom, A. B. Sieval, J. C. Hummelen, *J. Phys. Chem. A* **2005**, *109*, 5266.
[33] A. Köhnen, M. Irion, M. C. Gather, N. Rehmann, P. Zacharias, K. Meerholz, *J. Mater. Chem.* **2010**, *20*, 3301.
[34] L. S. Hung, C. W. Tang, M. G. Mason, *Appl. Phys. Lett.* **1997**, *70*, 152.
[35] G. E. Jabbour, Y. Kawabe, S. E. Shaheen, J. F. Wang, M. M. Morrell, B. Kippelen, N. Peyghambarian, *Appl. Phys. Lett.* **1997**, *71*, 1762.
[36] S. E. Shaheen, G. E. Jabbour, M. M. Morrell, Y. Kawabe, B. Kippelen, N. Peyghambarian, M.-F. Nabor, R. Schlaf, E. A. Mash, N. R. Armstrong, *J. Appl. Phys.* **1998**, *84*, 2324.
[37] H. W. Choi, S. Y. Kim, W.-K. Kim, J.-L. Lee, *Appl. Phys. Lett.* **2005**, *87*, 082102.